Helmholtz-Zentrum
Geesthacht
Zentrum für Material- und Küstenforschung

Final Draft
of the original manuscript:

Wilmers, J.; Bargmann, S.:
Simulation of non-classical diffusion in polymers
In: Heat and Mass Transfer (2014) Springer

DOI: 10.1007/s00231-014-1365-6

Heat and Mass Transfer manuscript No.
(will be inserted by the editor)

Simulation of Non-Classical Diffusion in Polymers

Jana Wilmers · **Swantje Bargmann**

Received: date / Accepted: date

Abstract The present contribution is concerned with the computational modelling of non-classical diffusion in amorphous polymers. Special attention is paid to the limiting case of Case II diffusion. Application of the dual-phase-lag concept to Fick's first law leads to a description of Case II behaviour. The change in material properties during the glass transition is explicitly accounted for by a concentration dependent formulation of the material parameters.

The proposed model is well suited for modelling the sharp diffusion front and linear uptake kinetics associated with Case II diffusion. Application of a concentration dependent diffusion coefficient reduces the concentration gradient behind the front to a minimum. For the solution procedure, a finite element scheme in space and a finite difference method in time are applied. Three-dimensional numerical results are presented for classical Fickian and non-classical Case II diffusion. This paper adds to the basic understanding of the computational modelling of the Case II diffusion phenomenon.

Keywords amorphous polymers · non-Fickian diffusion · Case II sorption

1 Introduction

Diffusion processes in polymers occur in a large number of technical fields, ranging from membrane filtration to applications in semiconductor lithography. The diffusion may be undesirable, but in many cases it is used deliberately, e.g., for microstructuring of polymer surfaces [1]. Other applications include photoresists [2], membranes [3] and controlled release drugs [4, 5]. This wide range of possible applications calls for a deep understanding of diffusion in polymers.

Classically, diffusion is described by Fick's laws, but in polymers at and below the glass transition temperature, non-Fickian behaviour is regularly encountered. These anomalies are attributed to relaxation within the polymer, which is necessary to admit the solvent into the molecular network. A considerable macroscopic swelling accompanying the diffusion of vapours and liquids into polymers is the result of this rearrangement.

In systems exhibiting Fickian diffusion, relaxation takes place so fast that it can be considered instantaneous. Especially in glassy polymers, however, relaxation occurs much slower and, thus, can inhibit the diffusion process. The limiting case, in which relaxation rates are much slower than the solvent mobility and consequently determine the diffusion kinetics, is called Case II diffusion. Here, the relaxation hinders the solvent uptake and, thus, causes the formation of a characteristic sharp diffusion front that propagates with a constant velocity in a wave-like manner through the specimen.

This front results in steep concentration and stress profiles. In addition, the coupling between diffusion and deformation is very strong, which renders the modelling of Case II behaviour a challenging task. In the past centuries, a large number of theoretical models describing Case II diffusion have been developed, most of them under the limiting assumption of infinitesimal deformation. A few prominent examples are presented in Section 2. For a more detailed overview of diffusion in polymers - experimental as well as modelling approaches - the reader is referred to, e.g., the review papers [6–8] and references therein. The textbook by

J. Wilmers
Institute of Materials Research, Materials Mechanics, Helmholtz-Zentrum Geesthacht, D-21502 Geesthacht, Germany
E-mail: jana.wilmers@hzg.de

S. Bargmann
Institute of Continuum and Material Mechanics, Hamburg University of Technology, D-21073 Hamburg, Germany

Institute of Materials Research, Materials Mechanics, Helmholtz-Zentrum Geesthacht, D-21502 Geesthacht, Germany

Crank [9] gives not only a comprehensive introduction to the mathematical description of Fickian diffusion but also an insight into non-Fickian behaviour and other special diffusion processes.

In the present contribution, a formulation of Case II behaviour based on a dual phase-lag approach originally suggested for high rate heating [10] is proposed. Choosing a formulation that is analogous to heat conduction stands to reason as Fick's 1st law is of the same mathematical structure as Fourier's law of heat flow.

To illustrate the suitability of the proposed approach, comparative three-dimensional simulations of Fickian and Case II diffusion are presented. An in-house C++ code is used to implement and solve the equations for pure diffusion numerically. In Section 2, a brief review of the current state of research regarding the diffusion process of Case II is given and its characteristic features are described. The chosen mathematical formulation is presented in Section 3. Subsequently, the discretisation in space and time is described. The numerical examples and their results are presented in Section 4.2. Finally, the results are discussed and conclusions are given.

2 Case II diffusion in solid polymers

The term Case II diffusion was coined by Alfrey et al. in 1966 [11]. There exists a large number of earlier experimental works, e.g. [12–15], describing deviation from Fickian behaviour for diffusion of comparatively small molecules in glassy polymers and the sharp diffusion fronts and large swelling accompanying it. Based on their own experimental work, Alfrey et al. introduced Case II diffusion as a limiting case for extremly non-Fickian conditions and gave the first systematic description of the process.

Case II diffusion exhibits solvent penetration at a constant velocity with a well-defined, sharp front. By increasing the molecular mobility considerably, the penetrant causes the solid to undergo plasticisation, i.e., a transition from the glassy to a rubber-like state. The plasticisation is associated with large macroscopic deformations, i.e., swelling of the polymer. Swelling and relaxation take place at a finite rate that for Case II diffusion is significantly slower than the diffusion. Due to this imbalance, the relaxation hinders the solvent uptake and, therefore, is the rate-controlling process. The delayed uptake causes the formation of a characteristic sharp diffusion front with constant propagation velocity.

Behind this front, the swollen polymer is in an equilibrium state, due to the fact that the diffusion kinetics are much faster than the relaxation. This manifests in a constant concentration behind the front and, thus, in a step-like concentration profile.

The constant propagation velocity is equivalent to a mass uptake which is linear in time. Describing the mass uptake over time $m(t)$, normalised by the equilibrium mass uptake m_∞, by

$$\frac{m(t)}{m_\infty} = k t^n , \tag{1}$$

with k as an arbitrary constant, allows to differentiate between different types of diffusional behaviour, see e.g. [11]. For Case II diffusion, the exponent n takes the value of 1, while for Fickian diffusion it is equal to 0.5. Diffusion in the range $0.5 < n < 1$ is termed "anomalous diffusion" (see e.g. [6]) and occurs for systems in which relaxation and diffusion time are of the same order. These values for the exponent n are only valid for diffusion in a slab. The effect of other geometries on the power law, i.e. Eq. (1), have been investigated in [16, 17]. In [18], Peppas and Sahlin reformulated the power law to reveal the superimposed contributions of Fickian and Case II transport in anomalous diffusion behaviour.

While the distinction between anomalous behaviour and Fickian or Case II is in some case clearly visible, cf. the linear concentration profiles measured in [19], in other cases, anomalous diffusion may exhibit some of the characteristic features of Case II diffusion. In [20], for example, the polymer swells due to the solvent uptake but the concentration profiles show no front formation. On the other hand, in [21], the experimentally obtained concentration profiles reveal a sharp front but are not step-like, while in [22] an equilibrium concentration plateau is reached but it is accompanied by a considerably broadened front. To classify the behaviour of a given polymer-solvent sample as Case II, all of the characteristics have to be visible, namely a sharp front with a constant velocity, a step-like concentration profile and swelling of the polymer.

The relation of relaxation rate and penetrant mobility determines the kind of diffusive behaviour a polymer-penetrant system exhibits. As a consequence, Vrentas et al. [23, 24] introduced the diffusional Deborah number *De* as a parameter to characterise diffusion. The Deborah number is defined as

$$De = \frac{\tau}{t_c} , \tag{2}$$

where τ denotes the relaxation time and t_c is the characteristic diffusion time. For Case II diffusion $De = \mathcal{O}(1)$, indicating the dominating nature of relaxation.

Both, the relaxation time and the characteristic diffusion time, depend on a large number of factors, such as temperature, steric effects, polymer-penetrant interaction or thermal and mechanical history [6]. Depending on these factors, a given polymer-penetrant system exhibits different types of diffusion. Thus, for temperatures well above the glass transition temperature T_g of the mixture, Fickian diffusion occurs in an amorphous polymer, while below T_g, anomalous and Case II behaviour is observed.

Since the first systematic description of Case II diffusion, numerous experimental studies have been carried out, observing Case II behaviour in different polymers, including the widely used poly(methyl methacrylate) [3, 25, 26] and polystyrene [27, 28], among others [1, 29, 30].

In addition to these experimental works, there has been considerable effort in the development of a theoretical model describing Case II diffusion. The first model taking the coupling between diffusion and swelling into account was introduced by Thomas and Windle [31, 32]. This model explicitly considers the osmotic pressure caused by penetration being responsible for the viscous response of the polymer. In contrast to Fickian diffusion, the gradient of the chemical potential is regarded as the driving force for diffusion. This approach is pursued in the vast majority of later models.

Durning et al. [33] used the Maxwell viscoelastic model instead of the viscous one suggested by Thomas and Windle and derived a model for differential sorption from thermodynamical considerations that incorporates the Thomas-Windle model as a special case for small Deborah numbers [34]. Wu et al. [35] extended Durning's model to integral sorption under assumption of ideal mixing and small deformations. Like the other presented models, this framework is limited to one spatial dimension.

The model presented in [36] follows a different approach. It is based on a seperation of the diffusive flux into a sum of different contributions, each with their own relaxation time. The model qualitatively describes transport with Fickian and Case II as well as intermediate, anomalous behaviour.

A more general formulation of Case II diffusion was introduced by Govindjee and Simo [37]. Their model is thermodynamically consistent and formulated within the framework of nonlinear continuum mechanics. Basic balance equations are used to describe the motion of the mixture and the diffusive behaviour of the solvent, while the free energy is calculated using information about the system's microstructure. The model accounts for the viscoelastic material response as well as for the large deformations occuring during Case II diffusion. In [37] the authors show that their model is able to reproduce the characteristics of Case II diffusion for the example of a traction free slab. Based on the work by Govindjee and Simo [37], McBride et al. [38, 39] derived a continuum thermomechanical framework for non-Fickian diffusion that can be specialised for Case II by an appropriate formulation of the Helmholtz free energy. In this framework, inelastic deformation is coupled to diffusion and heat conduction and surface effects are accounted for. In our previous work [40], this general framework is developed in the configurational setting of continuum mechanics.

The strong coupling and the steep profiles in stresses and concentrations are sources of possible instabilities in numerical simulations of Case II diffusion. Therefore, particular care has to be put into the numerical treatment and concurrently few thorough numerical studies are to be found in the literature. In [41], Wu et al. describe a finite difference scheme for simulations of the method introduced in [35]. This approach is reviewed by Vijalapura et al. in [42, 43] and deficiencies in the solution procedure are addressed. Furthermore, Vijalapura et al. propose a numerical procedure for the solution of Govindjee and Simo's method [37]. For spatial discretisation, a finite element approach is used and an adaptive finite difference scheme is formulated with great rigour for time discretisation.

Wang et al. [44] follow the works of Govindjee and Simo [37] and McBride et al. [39] to include viscoelastic behaviour into the modelling of polymeric gels and present examples of numerical simulations. However, their work does not concern anomalous diffusion. Similarily, in [45], the coupling of diffusion and large deformations is modelled and simulated without consideration of anomalous behaviour. A recent contribution regarding the coupling between large deformations in amorphous polymers and temperature is presented in [46, 47].

3 Mathematical description of diffusion

In 1855, Fick [48] published the results of his investigation of diffusion in which he proposes the diffusive flux $\mathbf{j}$ to be proportional to the concentration gradient

$$\mathbf{j}(\mathbf{x},t) = -\mathsf{D}(\mathbf{x}) \cdot \nabla c(\mathbf{x},t)\,, \tag{3}$$

where D is the second order diffusion coefficient tensor and c denotes concentration. The nabla operator ∇ represents a gradient in space. Assuming that diffusing particles are neither destroyed nor created (e.g., by chemical reactions) allows to express the conversation of diffusing species mass as

$$\frac{\partial c}{\partial t} + \operatorname{div}\mathbf{j} = 0\,. \tag{4}$$

Applying this continuity equation to Fick's 1st law, Eq. (3), gives

$$\dot{c} = \operatorname{div}(\mathsf{D} \cdot \nabla c)\,, \tag{5}$$

where div is the divergence operator and the superscript $\dot{\bullet}$ denotes the time derivative.

The diffusion coefficient D is a scalar constant for isotropic materials like amorphous polymers. In this case, Eq. (5) is reduced to Fick's 2nd law

$$\dot{c} = D \operatorname{div}\nabla c\,. \tag{6}$$

Fick's laws have the drawback of mapping an instantaneous information propagation. In addition, this formulation is insufficient for the description of Case II behaviour. To counteract this drawback, it seems natural to replace the

parabolic Eq. (6) by a hyperbolic one (cf. [49]) and, thus, introduce a finite propagation velocity. The drawback of infinite propagation speed and the lack of possibilities to capture certain non-classical effects is also known for Fourier's theory of heat conduction [50], see e.g. [51–56].

For heat conduction, a number of approaches addressing the finite propagation speed use hyperbolic or hyperbolic-like equations, cf. e.g. [55, 56]. The first, and probably most well known, of these approaches was published independently by Maxwell [57], Cattaneo [58] and Vernotte [59].

Another approach is the dual-phase-lag model [10, 60, 61] which was developed for description of the microstructural effects during rapid heating causing wave-like heat conduction. In [62] the dual-phase-lag model is transferred to layer growth, a process involving species diffusion and chemical reactions. In the present contribution, we apply the dual-phase-lag concept to the description of Case II diffusion.

The diffusion in glassy polymers is hindered by interactions of the solvent with the polymer molecules and relaxation processes within the polymer. In the context of the dual-phase-lag approach, these molecular effects are interpreted as causing a lagging response in the diffusion behaviour, which gives

$$\mathbf{j}(\mathbf{x},t+\tau_j) = -D(c)\,\nabla c(\mathbf{x},t+\tau_c)\,, \tag{7}$$

where the positive relaxation times τ_j and τ_c represent the retardation of the diffusion flux and the delayed formation of the concentration gradient, respectively. These relaxation times are intrinsic properties of the considered polymer-solvent system.

Equation (7) is expanded by a Taylor series. Keeping in mind that a change of the unit systems should not change the constitutive relations, a first order approximation is sufficient:

$$\mathbf{j}(\mathbf{x},t) + \tau_j \frac{\partial\,\mathbf{j}(\mathbf{x},t)}{\partial t} = -D(c)\,\nabla c(\mathbf{x},t) - \tau_c D(c) \frac{\partial \nabla c(\mathbf{x},t)}{\partial t}\,. \tag{8}$$

In combination with the continuity equation (4), this yields the following diffusion law

$$\dot{c} + \tau_j\,\ddot{c} = \operatorname{div}(D(c)\,\nabla c) + \tau_c \operatorname{div}(D(c)\,\nabla \dot{c}). \tag{9}$$

For $\tau_j = \tau_c = 0$, this equation reduces to Fick's 2$^{\text{nd}}$ law and for $\tau_j > 0$ and $\tau_c = 0$, Eq. (9) is the same as the Maxwell-Cattaneo-Vernotte approach applied to species diffusion.

The glass transition inherent in Case II diffusion is associated with considerable changes in the material which in turn manifest in changes of the material constants. Ahead of the diffusion front, the polymer is still glassy and thus the relaxation times τ_j and τ_c are high and the diffusion coefficient D is low, while behind the front, relaxation and diffusion become faster. The change of the diffusion coefficient during anomalous diffusion has been investigated in [15] for different halocarbons in polystyrene and is shown to follow $D = D_0 \exp(\alpha\, v)$, where the underlying diffusion coefficient D_0 and the parameter α are constants for any polymer-penetrant system at constant temperature and v is the penetrant volume fraction. Due to the constant density of the pure penetrant, the concentration may be used instead of the volume fraction

$$D = D_0 \exp(\alpha\, c)\,. \tag{10}$$

This formulation of the concentration dependence is applicable for different polymers, cf. [35]. The concentration dependence of the retardation times can be formulated in a similar manner

$$\tau_j = \tau_{j0} \exp(-\beta\, c) \qquad \text{and} \qquad \tau_c = \tau_{c0} \exp(-\beta\, c)\,. \tag{11}$$

Here, τ_{j0} and τ_{c0} denote the base values of the relaxation times and β is the factor determining the range of variation.

4 Numerical examples

4.1 Numerical treatment

For the discretisation of Equations (6) and (9) the method of lines is used. First, the equations are discretised in space with the finite element method. The resulting time-dependent equations are solved by application of a temporal finite difference scheme. In the following, details of this treatment are presented.

The weak forms for Fickian and Case II diffusion are obtained by multiplication with a test function δc and integration over the volume

$$\int_V \delta c\, \dot{c}\, \mathrm{d}V = D \int_V \delta c \operatorname{div} \nabla c\, \mathrm{d}V\,, \tag{12}$$

$$\begin{aligned} \int_V \delta c\, [\dot{c} + \tau_j(c)\ddot{c}]\, \mathrm{d}V = \int_V \delta c\, [&\operatorname{div}(D(c)\,\nabla c) \\ &+ \operatorname{div}(\tau_c(c)\, D(c)\, \nabla \dot{c})]\, \mathrm{d}V\,. \end{aligned} \tag{13}$$

The right hand sides of Equations (12) and (13) are integrated by parts. Utilising Gauß's theorem yields , with $\mathbf{n}$ being the normal vector field of the boundary ∂V,

$$\begin{aligned} \int_V \delta c D \operatorname{div} \nabla c\, \mathrm{d}V = &- \int_V D \nabla \delta c \cdot \nabla c\, \mathrm{d}V \\ &+ \int_{\partial V} D \delta c \nabla c \cdot \mathbf{n}\, \mathrm{d}A\,, \end{aligned} \tag{14}$$

$$\begin{aligned} &\int_V \delta c\, [\operatorname{div}(D(c) \nabla c) + \operatorname{div}(\tau_c(c)\, D(c) \nabla \dot{c})]\, \mathrm{d}V \\ &\quad = - \int_V D(c) \nabla \delta c \cdot [\nabla c + \tau_c(c)\, \nabla \dot{c}]\, \mathrm{d}V \\ &\qquad + \int_{\partial V} D(c)\, \delta c [\nabla c + \tau_c(c)\, \nabla \dot{c}] \cdot \mathbf{n}\, \mathrm{d}A\,. \end{aligned} \tag{15}$$

The volume is discretised into finite elements using a standard Galerkin-Bubnov approach, i.e., both the concentration c and the test function δc are approximated with the same, here linear, functions N^i over the n nodes, according to

$$c = \sum_{i=1}^{n} N^i c_i \,, \qquad \delta c = \sum_{i=1}^{n} N^i \delta c_i \,.$$

For the gradients of the concentration and the test functions, the following approximations are applied

$$\nabla c = \sum_{i=1}^{n} \nabla N^i c_i \,, \qquad \nabla \delta c = \sum_{i=1}^{n} \nabla N^i \delta c_i \,.$$

Furthermore, the isoparametric concept is applied, so that the shape functions interpolating the geometry are equal to N^i.

The semi-discretised time-dependent system is solved with a finite difference scheme. The second derivative in time of the concentration is approximated by a second order central difference

$$\ddot{c} \approx \frac{\mathbf{c}^{j+1} - 2\mathbf{c}^{j} + \mathbf{c}^{j-1}}{\Delta t^2} \,, \tag{16}$$

while for the first derivative a backward Euler scheme is applied

$$\dot{c} \approx \frac{\mathbf{c}^{j} - \mathbf{c}^{j-1}}{\Delta t} \,. \tag{17}$$

Here, the superscript j denotes the current time step and Δt is the time step width. For better readability, the subscript marking the concentration $\mathbf{c}$ as a vector of nodal values is dropped.

The initial condition for Fickian behaviour, i.e., Eq. (6), reads

$$\mathbf{c}(\mathbf{x}, 0) = \mathbf{c_0}(\mathbf{x}) \,.$$

Accordingly, the initial conditions for Case II behaviour, i.e., Eq. (9), are chosen as

$$\mathbf{c}(\mathbf{x}, 0) = \mathbf{c_0}(\mathbf{x}) \qquad \text{and} \qquad \dot{\mathbf{c}}(\mathbf{x}, 0) = \mathbf{0} \,.$$

4.2 Model set-up

In order to test the applicability of the proposed approach for modelling of Case II diffusion and to compare it to Fick's law, numerical simulations are carried out. In this and the following sections, details of the implementation of Case II are given before the results for both diffusion mechanisms are compared. The diffusion of a fluorinated hydrocarbon (3,5-bis(trifluoromethyl)aniline) vapour into solid polystyrene is examined. The values for the diffusion coefficient ($D = 7.2 \cdot 10^{-10}\,\mathrm{cm^2/min}$) and the relaxation time ($\tau_j = 157.2\,\mathrm{min}$)

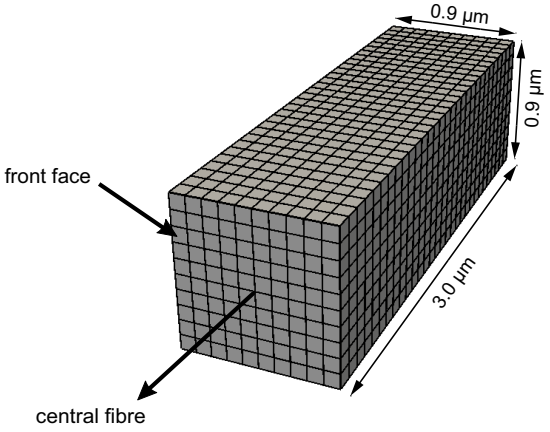

Fig. 1: Geometry of the specimen.
The specimen is discretised with brick elements. On the front face, a constant concentration is applied. A one-dimensional fibre is defined in the centre of the specimen for evaluation of the concentration profiles.

are taken from [27], where they were measured at a temperature of 295.65 K. The delay of gradient formation is set to $\tau_c = 6.3\,\mathrm{min}$, such that it is considerably smaller than τ_j. This restriction is due to the fact that the experiments (e.g. [28]) show that the delay of the flux dominates the behaviour of Case II diffusion. Because of the choice $\tau_j \gg \tau_c$, Eq. (9) is essentially a Maxwell-Cattaneo-Vernotte-like model.

The basic geometry of the polystyrene specimen is depicted in Fig. 1. It is cuboidal, with length $l = 3\,\mu\mathrm{m}$, height $h = 0.9\,\mu\mathrm{m}$ and width $w = 0.9\,\mu\mathrm{m}$, and it is discretised using 3,000 cubical finite elements. For $l = 3\,\mu\mathrm{m}$, the Deborah number *De*, which is defined in Eq. (2) with the characteristic time $t_c = l^2/D$, is 1.258 and, therefore, the system exhibits Case II behaviour.

For this example, a constant concentration c_∞ is specified at the front face of the specimen (see Fig. 1). At all boundaries, the flux over the surface is assumed to vanish (cf. Section 4.1). The concentration within the specimen is given as the normalised concentration $c = c(x,t)/c_\infty$. These boundary conditions represent the specimen being in contact with a large reservoir of the penetrant, as is schematically shown in Fig. 2

4.3 Concentration dependence

The concentration dependence of the constants D, τ_j and τ_c is described using the exponential laws introduced in Equations (10) and (11). This continuous change in the properties is preferable to a sudden change in parameters at a given concentration because it complies with the physical process of glass transition. The glass transition is not a phase tran-

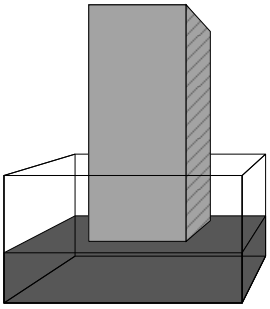

Fig. 2: Illustration of the model set-up.
A polymer slab is on one face in contact with a large reservoir of the penetrant.

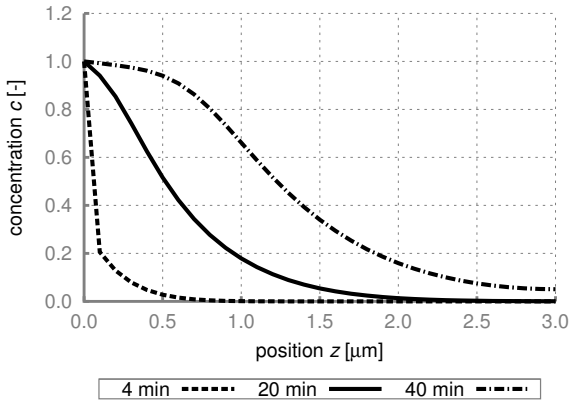

Fig. 3: Case II diffusion: Comparison of the concentration profiles at different times, neglecting the concentration dependence of the material parameters.
The diffusion front broadens with time.

sition but a kinetic phenomenon occurring over a range of temperatures. Material properties like the viscosity or the heat capacity change smoothly in this range, thus, a smooth change in the diffusion coefficient and the relaxation times is to be expected.

The experimental values given in [27] are considered as mean values for the system. Hence, they are adopted as the values for a normalised concentration of $c = 0.5$. The factor α in Eq. (10) is chosen to be 5 so that the diffusion coefficient changes over a realistically large range of over two orders of magnitude. The change in the relaxation times is smaller; with $\beta = 1.5$ in Eq. (11), the value $\tau_j(c = 1.0)$ is 4.5 times larger than $\tau_j(c = 0.0)$.

Incorporating $D(0.5) = 7.2 \cdot 10^{-10}\,\mathrm{cm}^2/\mathrm{min}$, $\tau_c(0.5) = 157.2\,\mathrm{min}$ and $\tau_c(0.5) = 6.3\,\mathrm{min}$ gives

$$D(c) = 7.2 \cdot 10^{-10}\,\mathrm{cm}^2/\mathrm{min} \cdot \exp(5 \cdot [c - 0.5])\,, \tag{18}$$

$$\tau_j(c) = 157.2\,\mathrm{min} \cdot \exp(-1.5 \cdot [c - 0.5])\,. \tag{19}$$

and

$$\tau_c(c) = 6.3\,\mathrm{min} \cdot \exp(-1.5 \cdot [c - 0.5])\,. \tag{20}$$

To illustrate the effect that the concentration dependence of the material parameters has, Fig. 3 shows the concentration profile over the one dimensional ‘central fibre’ of the cuboidal specimen (see Fig 1) for $D = \text{const}$, $\tau_j = \text{const}$ and $\tau_c = \text{const}$. In comparison, Fig. 4 depicts the solutions of Eq. (9) including the concentration dependence.

Fig. 4a shows the behaviour with the described concentration dependencies. Ahead of the front, a small divergence in the concentration profile appears as it does in Fig. 4b. This divergence is known as the Fickian precursor, a small amount of penetrant that is admitted into the free volume in the un-relaxed polymer ahead of the front. This phenomenon is experimentally visible in Case II diffusion, cf. e.g. Thomas et al. [31]. In Fig. 4 a change in the diffusion velocity in comparison with Fig. 3 is apparent. This behaviour is due to the differing material constants.

A comparison of Figures 3 and 4a shows that the front becomes steeper if the concentration dependence is taken into account. In particular, this effect is distinct for longer observation times.

In addition to the narrowing of the front, the concentration gradient increases behind the front in Fig. 4a. Diffusion profiles like this one are known from anomalous diffusion experiments experiments, cf. [21]. In experiments of Case II diffusion, however, almost no gradient in concentration is observed behind the front, cf. [63]. If the diffusion coefficient is assumed to be concentration dependent and the relaxation times are kept constant, the gradient behind the front vanishes (see Fig. 4b).

4.4 Comparison between Fick and Case II

For both, Fickian and Case II diffusion, the same sample geometry is investigated. The cuboidal specimen is discretised by 3000 brick elements. 1000 equidistant time steps are considered.

In accordance with the results of the previous section, for Case II, the relaxation times are assumed independent of the concentration and for the diffusion coefficient, Eq. 18 is employed. For Fickian diffusion, a constant diffusion coefficient $D = 8.7714 \cdot 10^{-9}\,\mathrm{cm}^2/\mathrm{min}$ is chosen. This value is identical to $D(c = 1.0)$ for Case II.

Different diffusion types may be defined by consideration of their uptake kinetics, as described in Section 2. In Fig. 5, the mass uptake for both investigated theories is depicted. Fickian diffusion shows the expected proportionality to $\sqrt{t}$, while the uptake for Case II is clearly linear in time. In the beginning of Case II diffusion, a small deviation from the linear behaviour related to the establishing of the front occurs.

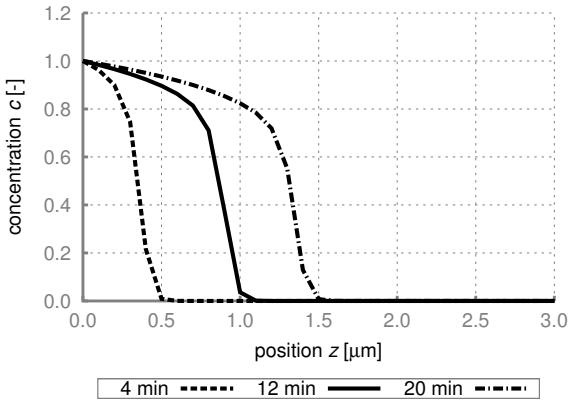

(a) using $D(c)$, $\tau_j(c)$ and $\tau_c(c)$

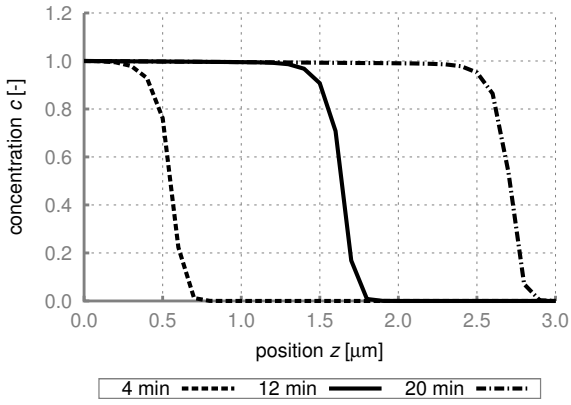

(b) using $D(c)$, $\tau_j = \text{const}$ and $\tau_c = \text{const}$

Fig. 4: Case II diffusion: Influence of concentration dependent material parameters on the concentration profile.
(a) Considering the concentration dependence steepens the front but increases the gradient behind it. (b) With constant relaxation times, the gradient behind the front is minimised.

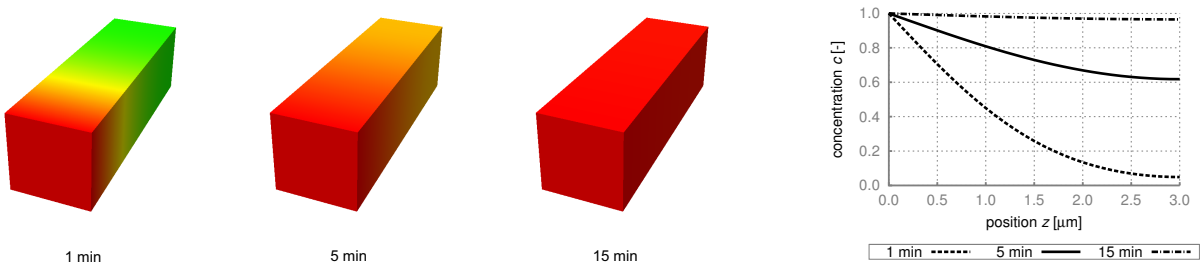

Fig. 6: Fickian diffusion.
A smooth concentration gradient that flattens with time is established.

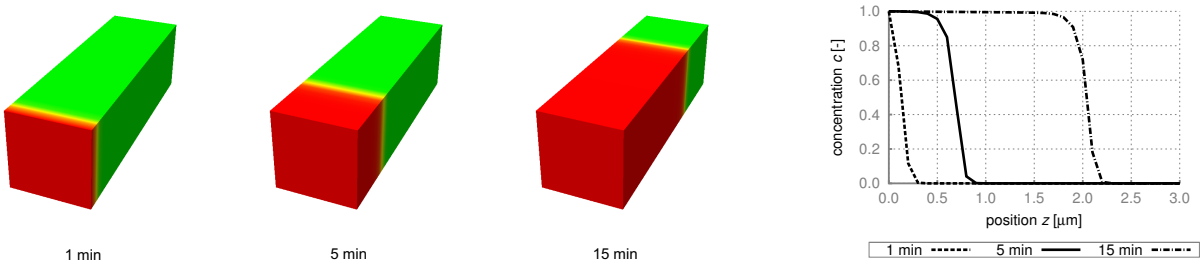

Fig. 7: Case II diffusion.
The characteristic front is upheld for the whole diffusion process and moves at a constant velocity through the specimen.

Besides the linear mass uptake kinetics, the most important characteristic of Case II diffusion is the sharp diffusion front. In Figures 6 and 7, the solutions for Fick and Case II are depicted for the whole specimen at three different time steps. The different propagation speeds of Fickian and Case II diffusion are clearly visible. Figure 6 shows the typical smooth gradients caused by balancing of the difference in concentration between both ends of the specimen. The sharp front and its wave-like propagation through the specimen are clearly visible in Fig. 7 for all time steps. Behind the front, no gradient occurs.

As expected, Fick's law is inapplicable to model Case II diffusion, as the concentration does not propagate as a wave. However, the discretisation approach suggested in Section 4.1

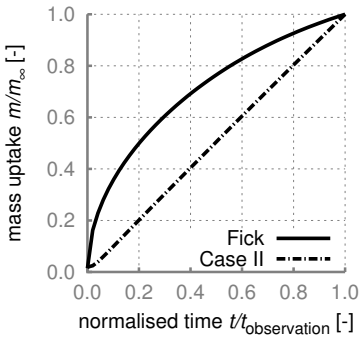

Fig. 5: Normalised mass uptake over normalised time.
For better comparison of both mechanisms, mass uptake and time are normalised with respect to their values once a homogeneous concentration is achieved. The mass uptake for Fickian diffusion is proportional to $\sqrt{t}$, whereas for Case II it is proportional to t.

works well for the classical as well as for the non-classical theory. The mathematical model for Case II diffusion as proposed in this article (based on the dual-phase-lag concept [10] and related to the well known Maxwell-Cattaneo-Vernotte approach [57–59]) yields a very good qualitative agreement with Case II propagation behaviour as observed in experiments. As is evident in Fig. 5, the model exhibits the linear uptake kinetics described already by Alfrey [11] and observed experimentally, e.g., in [63, 64]. The concentration profile depicted in Fig. 4b has a very distinct step-form with a sharp front, which is characteristic for Case II diffusion as shown experimentally by Stamatialis and coworkers using microinterferometry [63]. For non-Case II anomalous diffusion the concentration profiles differ strongly from this step-form, cf. [21, 22].

5 Conclusion

This article deals with non-Fickian diffusion in glassy polymers, especially with the limiting case Case II diffusion. The significant coupling between species transportation and deformation displayed in Case II behaviour was neglected in favour of modelling and studying of pure diffusion. To this end, a dual-phase-lag approach was used in three-dimensional simulations of Case II. The results of this approach were compared with those of Fickian diffusion to emphasise the differences between the diffusive behaviours. A combination of finite element and finite difference schemes was used in the simulations of a generic example volume. To account for the changes in the material associated with Case II diffusion, the diffusion coefficient and the relaxation times were described as concentration dependent. Taking the concentration dependence into account resulted in an increased steepness of the characteristic diffusion front. This, however, also caused a more prominent concentration gradient behind the front. Choosing only the diffusion coefficient to be dependent on the concentration resolved this issue. In fact, the gradient behind the front vanished almost completely.

It was demonstrated that the proposed model was able to describe the characteristic features of Case II diffusion. The model predicts a step-like concentration profile with a sharp front that moves at a constant, finite velocity as is evident from the linear uptake kinetics.

References

1. Rahmanian O, Chen CF, DeVoe DL (2012) Microscale patterning of thermoplastic polymer surfaces by selective solvent swelling. Langmuir 28(35):12923–12929
2. Mills PJ, Kramer EJ (1989) Debonding of photoresist caused by Case II diffusion. Journal of Materials Science 24(2):439–446
3. Hori K, Matsuno H, Tanaka K (2011) Sorption kinetics of methanol in thin poly(methyl methacrylate) films studied by optical reflectivity. Soft Matter 7(21):10319–10326
4. Liu S, Jiang M, Ye S, Xu X, Lu P, Dong J (2012) Biodegradable poly(glycerin citrate) and its application to controlled release of theophylline. Journal of Applied Polymer Science 124(5):3633–3640
5. Singh B, Pal L (2012) Sterculia crosslinked PVA and PVA-poly(AAm) hydrogel wound dressings for slow drug delivery: Mechanical, mucoadhesive, biocompatible and permeability properties. Journal of the Mechanical Behavior of Biomedical Materials 9(0):9–21
6. De Kee D, Liu Q, Hinestroza J (2005) Viscoelastic (non-fickian) diffusion. The Canadian Journal of Chemical Engineering 83(6):913–929
7. Vesely D (2008) Diffusion of liquids in polymers. International Materials Reviews 53(5):299–315
8. Bargmann S, McBride AT, Steinmann P (2011) Models of solvent penetration in glassy polymers with an emphasis on Case II diffusion. A comparative review. Applied Mechanics Reviews 64(1):010803–1 – 010803–13
9. Crank J (1975) The Mathematics of Diffusion. 2nd edition. Oxford science publications, Clarendon Press
10. Tzou DY (1995) A unified field approach for heat conduction from macro- to micro-scales. Journal of Heat Transfer 117(1):8–16. 10.1115/1.2822329
11. Alfrey T, Gurnee EF, Lloyd WG (1966) Diffusion in glassy polymers. Journal of Polymer Science Part C: Polymer Symposia 12(1):249–261
12. Hartley GS (1949) Diffusion and swelling of high polymers. Part III.-anisotropic swelling in oriented polymer film. Transactions of the Faraday Society 45(0):820–832

13. Crank J, Park GS (1949) An evaluation of the diffusion coefficient for chloroform in polystyrene from simple absorption experiments. Transactions of the Faraday Society 45(0):240–249
14. Crank J, Park GS (1951) Diffusion in high polymers: some anomalies and their significance. Transactions of the Faraday Society 47(0):1072–1084
15. Park GS (1951) The diffusion of some organic substances in polystyrene. Transactions of the Faraday Society 47(0):1007–1013
16. Ritger PL, Peppas NA (1987) A simple equation for description of solute release i. fickian and non-fickian release from non-swellable devices in the form of slabs, spheres, cylinders or discs. Journal of Controlled Release 5(1):23 – 36
17. Ritger PL, Peppas NA (1987) A simple equation for description of solute release ii. fickian and anomalous release from swellable devices. Journal of Controlled Release 5(1):37 – 42
18. Peppas NA, Sahlin JJ (1989) A simple equation for the description of solute release. iii. coupling of diffusion and relaxation. International Journal of Pharmaceutics 57(2):169 – 172
19. Cascone S, Lamberti G, Titomanlio G, dAmore M, Barba AA (2014) Measurements of non-uniform water content in hydroxypropyl-methyl-cellulose based matrices via texture analysis. Carbohydrate Polymers 103:348–354
20. Chirico S, Dalmoro A, Lamberti G, Russo G, Titomanlio G (2007) Analysis and modeling of swelling and erosion behvior for pure hpmc tablet. Journal of Controlled Release 122:181–188
21. Ekenseair AK, Ketcham RA, Peppas NA (2012) Visualization of anomalous penetrant transport in glassy poly(methyl methacrylate) utilizing high-resolution x-ray computed tomography. Polymer 53(3):776–781
22. Barba AA, d'Amore M, Chirico S, Lamberti G, Titomanlio G (2009) Swelling of cellulose derivative (hpmc) matrix systems for drug delivery. Carbohydrate Polymers 78:469–474
23. Vrentas JS, Jarzebski CM, Duda JL (1975) A Deborah number for diffusion in polymer-solvent systems. AIChE Journal 21(5):894–901
24. Vrentas JS, Duda JL (1977) Diffusion in polymersolvent systems. III. Construction of Deborah number diagrams. Journal of Polymer Science: Polymer Physics Edition 15(3):441–453
25. Stamatialis DF, Sanopoulou M, Raptis I (2002) Swelling and dissolution behavior of poly(methyl methacrylate) films in methyl ethyl ketone/methyl alcohol mixtures studied by optical techniques. Journal of Applied Polymer Science 83(13):2823–2834
26. Li JX, Lee PI (2006) Effect of sample size on Case II diffusion of methanol in poly(methyl methacrylate) beads. Polymer 47(22):7726–7730
27. Umezawa K, Gibson WM, Welch JT, Araki K, Barros G, Frisch HL (1992) A study of Case II diffusion of a fluorinated hydrocarbon in poly(styrene) by resonance nuclear reaction analysis. Journal of Applied Physics 71(2):681–684
28. Ogieglo W, Wormeester H, Wessling M, Benes NE (2013) Temperature-induced transition of the diffusion mechanism of n-hexane in ultra-thin polystyrene films, resolved by in-situ spectroscopic ellipsometry. Polymer 54(1):341–348
29. Hopkinson I, Jones RAL, Black S, Lane DM, McDonald PJ (1997) Fickian and Case II diffusion of water into amylose: A stray field NMR study. Carbohydrate Polymers 34(12):39–47
30. Fink D, Vacik J, Cervena J, Hnatowicz V, Kobayashi Y, Hishita S, Ghosh S, Klett R (1998) On the uptake of aqueous tracer solutions by pristine and ion-irradiated peek. Nuclear Instruments and Methods in Physics Research Section B: Beam Interactions with Materials and Atoms 134(1):61–72
31. Thomas NL, Windle AH (1980) A deformation model for Case II diffusion. Polymer 21(6):613–619
32. Thomas NL, Windle AH (1982) A theory of Case II diffusion. Polymer 23(4):529–542
33. Durning CJ, Tabor M (1986) Mutual diffusion in concentrated polymer solutions under a small driving force. Macromolecules 19(8):2220–2232
34. Fu TZ, Durning CJ (1993) Numerical simulation of Case II transport. AIChE Journal 39(6):1030–1044
35. Wu JC, Peppas NA (1993) Modeling of penetrant diffusion in glassy polymers with an integral sorption Deborah number. Journal of Polymer Science Part B: Polymer Physics 31(11):1503–1518
36. Camera-Roda G, Sarti GC (1990) Mass transport with relaxation in polymers. AIChE Journal 36(6):851–860
37. Govindjee S, Simo JC (1993) Coupled stress-diffusion: Case II. Journal of the Mechanics and Physics of Solids 41(5):863–887
38. McBride AT, Bargmann S, Steinmann P (2011) Geometrically Nonlinear Continuum Thermomechanics Coupled to Diffusion: A Framework for Case II Diffusion, Lecture Notes in Applied and Computational Mechanics, volume 59, book section 5, 89–107. Springer Berlin Heidelberg
39. McBride AT, Javili A, Steinmann P, Bargmann S (2011) Geometrically nonlinear continuum thermomechanics with surface energies coupled to diffusion. Journal of the Mechanics and Physics of Solids 59(10):2116–2133
40. Steinmann P, McBride AT, Bargmann S, Javili A (2012) A deformational and configurational framework for

geometrically non-linear continuum thermomechanics coupled to diffusion. Int J Non Linear Mech 47(2):13–13
41. Wu JC, Peppas NA (1993) Numerical simulation of anomalous penetrant diffusion in polymers. Journal of Applied Polymer Science 49(10):1845–1856
42. Vijalapura PK, Govindjee S (2003) Numerical simulation of coupled-stress Case II diffusion in one dimension. Journal of Polymer Science Part B: Polymer Physics 41(18):2091–2108
43. Vijalapura PK, Govindjee S (2005) An adaptive hybrid time-stepping scheme for highly non-linear strongly coupled problems. International Journal for Numerical Methods in Engineering 64(6):819–848
44. Wang X, Hong W (2012) A visco-poroelastic theory for polymeric gels. Proceedings of the Royal Society A 468(2148):3824–3841
45. Baek S, Srinivasa AR (2004) Diffusion of a fluid through an elastic solid undergoing large deformation. International Journal of Non-Linear Mechanics 39(2):201–218
46. Anand L, Ames NM, Srivastava V, Chester SA (2009) A thermo-mechanically coupled theory for large deformations of amorphous polymers. Part I: Formulation. International Journal of Plasticity 25(8):1474–1494
47. Ames NM, Srivastava V, Chester SA, Anand L (2009) A thermo-mechanically coupled theory for large deformations of amorphous polymers. Part II: Applications. International Journal of Plasticity 25(8):1495–1539
48. Fick A (1855) Ueber diffusion. Annalen der Physik 170(1):59–86
49. Kalospiros NS, Ocone R, Astarita G, Meldon JH (1991) Analysis of anomalous diffusion and relaxation in solid polymers. Industrial & Engineering Chemistry Research 30(5):851–864
50. Fourier JBJ (1822) Théorie analytique de la chaleur. Paris
51. Bargmann S, Steinmann P (2005) Finite element approaches to non-classical heat conduction in solids. Comp Model Eng Sci 9(2):133–150
52. Bargmann S, Steinmann P (2006) Theoretical and computational aspects of non-classical thermoelasticity. Computer Methods in Applied Mechanics and Engineering 196(13):516–527
53. Bargmann S, Steinmann P (2008) Modeling and simulation of first and second sound in solids. International Journal of Solids and Structures 45(24):6067–6073
54. Bargmann S, Steinmann P, Jordan PM (2008) On the propagation of second-sound in linear and non-linear media: Results from Green-Naghdi theory. Physics Letters A 372:4418–4424
55. Joseph DD, Preziosi L (1989) Heat waves. Reviews of Modern Physics 61(1):41–73
56. Joseph DD, Preziosi L (1990) Addendum to the paper “heat waves”. Reviews of Modern Physics 62(2):375–391
57. Maxwell JC (1867) On the dynamical theory of gases. Philosophical Transactions of the Royal Society of London 157:49–88
58. Cattaneo C (1948) Sulla conduzione del calore, 83–101. Università di Modena. Facoltà di scienze matematiche, fisiche e naturali, Modena
59. Vernotte P (1958) Les paradoxes de la théorie continue de l’équation de la chaleur. CR Acad Sci 246(22):3154–3155
60. Tzou DY (1995) The generalized lagging response in small-scale and high-rate heating. International Journal of Heat and Mass Transfer 38(17):3231–3240
61. Quintanilla R, Racke R (2006) A note on stability in dual-phase-lag heat conduction. International Journal of Heat and Mass Transfer 49(78):1209–1213
62. Chen JK, Beraun JE, Tzou DY (1999) A dual-phase-lag diffusion model for interfacial layer growth in metal matrix composites. Journal of Materials Science 34(24):6183–6187
63. Stamatialis DF, Sanopoulou M, Petropoulos JH (2002) Investigation of Case II diffusion behavior. 2. study of the poly(methylmethacrylate)-methyl alcohol system by two-beam microinterferometry. Macromolecules 35:1021–1027
64. Thomas N, Windle AH (1977) Transport of methanol in poly(methyl methacrylate). Polymer 19(3):255–265